TRA-04-0110.R1

Structure and Dynamics of the Golgi Complex at 15ºC: Low Temperature Induces the Formation of Golgi-derived Tubules

Emma Martínez-Alonso[1], Gustavo Egea[2], José Ballesta [1*], José A. Martínez-Menárguez[1*]

[1]Department of Cell Biology, School of Medicine, University of Murcia, 30100 Murcia, Spain

[2]Department de Biologia Cel.lular i Anatomia Patologica, Facultat de Medicina, IDIBAPS-Universitat de Barcelona, E-08036 Barcelona, Spain

Running title: The Golgi dynamics at low temperature

Key words: Golgi complex, ERGIC, membrane traffic, immunofluorescence, immunoelectron microscopy

[*]**Corresponding authors**:

José A. Martínez-Menárguez, jamartin@um.es; José Ballesta, ballesta@um.es. Phone number: 34-968398306, Fax number: 34-968-364323

ABSTRACT

Immunofluorescence and cryoimmunoelectron microscopy were used to examine the morphological and functional effects on the Golgi complex when protein transport is blocked at the ERGIC (ER-Golgi intermediate compartment) in HeLa cells incubated at low temperature (15ºC). At this temperature, the Golgi complex showed long tubules containing resident glycosylation enzymes but not matrix proteins. These Golgi-derived tubules also lacked anterograde (VSV-G) or retrograde (Shiga toxin) cargo. The formation of tubules was dependent on both energy and intact microtubule and actin cytoskeletons. Conversely, brefeldin A or cycloheximide treatments did not modify the appearance. When examined at the electron microscope, Golgi stacks were long and curved and appeared connected to tubules immunoreactive to galactosyltransferase antibodies but devoid of Golgi matrix proteins. Strikingly, COPI proteins moved from membranes to the cytosol at 15ºC which could explain the formation of tubules.

INTRODUCTION

The Golgi complex can be considered as the central station of the secretory pathway where newly synthesized proteins arrive from the endoplasmic reticulum (ER) and are sorted to their final destinations (1,2). In spite of this heavy membrane traffic, this organelle retains its characteristic morphology. Extensive studies have been carried out to identify the carriers, molecular mechanisms and regulators involved in transport throughout the secretory pathway. One milestone was the discovery that traffic of nascent proteins from ER to the Golgi involves a complex array of membranes located adjacent to the Golgi stack as well as multiple sites distributed throughout the cytoplasm (for review see 3-6). These elements have received different names, the most popular being vesicular tubular clusters (VTCs) and endoplasmic reticulum-Golgi intermediate compartment (ERGIC). The first name came from the morphological appearance of these elements. They consist of 0.2-1 μm clusters of small vesicles and short tubules apparently discontinuous with the ER and located at the cell periphery and the cis Golgi side (7). In contrast, the name "ERGIC" has more physiological implications and suggests a role as an obligatory step in the ER-Golgi transport (8,9). Current models postulate that the ERGIC originated by fusion of COPII-coated vesicles derived from the ER in both peripheral and central regions of the cell. Upon formation, this compartment moves to the Golgi stack guided by microtubules and matures en route by exchanging retrograde COPI-coated vesicles. Homotypic fusion of these carriers or their fusion with a pre-existing cisterna might be the origin of the first cis Golgi cisternae (5,10). Further steps on the secretory pathway are also under intense experimental research. Some of the current questions in this topic are the mode of intraGolgi transport (vesicular transport vs cisternal maturation) (11-14) and the dynamics of the Golgi at mitosis (template vs self-forming models) (15-17). The nature of the carriers that mediate all the steps of the route is also discussed. Small vesicles have been candidates for many years (18).

However, tubules and large pleomorphic membranes have been involved in some (or all) transport steps, including the retrograde Golgi-to-ER (19), ER-to-Golgi (20,21) and Golgi-to-plasma membrane pathways (22).

Newly synthesized secretory proteins accumulate in the ERGIC when cells are cultured at 15ºC (23,24). At this temperature the exit from the ERGIC is blocked. The blockade of the membrane traffic at the ERGIC for a long period may alter subsequent compartments such as the Golgi complex. A refined electron microscopical study of the distribution of the ERGIC marker protein p53 (from now on ERGIC-53) in hepatoma cells showed that it mainly concentrates at the ERGIC and moves from the periphery to the central region (25). Unexpectedly, no major alterations in the organization of the secretory pathway have been described. However, a detailed study of the structure and membrane dynamics of the Golgi complex at 15ºC has not been reported. Here we examine the effects of lowering temperature on the organization of the Golgi complex of HeLa cells using both immunofluorescence and quantitative cryoimmunolectron microscopy. We report a new type of Golgi-derived tubules which could mediate in the intraGolgi transport of glycosylation enzymes.

RESULTS

Low temperature induces the formation of tubules containing Golgi resident enzymes

Man II (26), GalTr (27) and GalNAcTr (28) are prototypical glycosylation enzymes, which are enriched in the medial, trans and all cisternae of the Golgi complex, respectively. At 37ºC, all three proteins showed the expected perinuclear Golgi staining pattern (Figures 1A and 3A). When cells were incubated at 15ºC, long Golgi-derived tubules extended to the cell periphery (Figures 1B and 3B). These tubules were morphologically similar to those induced by the treatment with brefeldin A (19). No difference was observed in the Golgi tubulation for the three

glycosylation enzymes, thus indicating that the whole Golgi stack is equally perturbed. Tubules appeared after 5 min in cells cultured at 15ºC, although the percentage of cells showing tubules was lower (64% for GalTr and 66% for GalNAcTr, Table I). Moreover, tubulation remained in cells cultured at 15ºC for up to 24 h. At this time point, the Golgi complexes appeared fragmented (data not shown). The number of tubules decreased significantly after rewarming the cells to 37ºC for short time (Table I). The low temperature-induced Golgi tubulation was also observed in Vero cells but not in HepG2 or NRK (data not shown) where, instead of tubule formation, low temperature induced a shift from a typical perinuclear compact distribution to a more punctate pattern, as described by Klumperman et al. (25). Low temperature-induced tubulation was not observed at the TGN, which was revealed with TGN-46 (data not shown).

Low temperature-induced Golgi tubules contain neither Golgi matrix proteins nor protein cargo

We next studied the content of the low temperature-induced tubules. The Golgi matrix protein GM130 and the integral membrane protein giantin are both part of a protein complex at the cis-Golgi side, which is apparently involved in vesicle tethering and cisternae stacking (29). At immunofluorescence level, GM130 (Figure 1C) and giantin (Figure 1E) showed a characteristic perinuclear labelling in control cells. When cells were incubated at 15ºC, this staining pattern remained virtually unaltered (Figures 1D and 1F, respectively). The same results were obtained with golgin-84 (data not shown), which is a recently identified member of the golgin family implicated in the generation and maintenance of the Golgi ribbon (30,31). These results suggest that these tubules did not contained Golgi matrix proteins.

We next examined whether the low temperature-induced tubules transported cargo. For this aim, we used two well-established cargo proteins: Shiga toxin and VSV-G protein. These proteins are

transported along the retrograde and the anterograde pathways, respectively. HeLa cells were incubated at 37ºC with cy3-tagged native Shiga toxin fragment B for 2 h, which accumulated in the Golgi complex. Thereafter, cells were incubated for several periods at 15ºC. The toxin colocalized with GalNAcTr (Figure 2A) but was excluded from the Golgi-derived tubules that contained only GalNAcTr (arrowheads in Figure 2A). Therefore, these double immunolabelling experiments show that the Shiga toxin as a retrograde cargo marker that constitutively cycles in the ER/Golgi interface do not enter these low temperature-induced tubules (Figure 2A merge). On the other hand, anterograde protein transport was monitored by using the temperature-sensitive mutant ts045 of the VSV-G. VSV-G protein transport from the ER to the Golgi was initiated by incubating the cells at the permissive temperature (32ºC) from the non-permissive temperature (40ºC). After 10 min at 32ºC, a significant portion of the viral protein reached the Golgi complex and then, cells were cultured at 15ºC, which induced the formation of Golgi-derived tubules. As occurred with Shiga toxin, VSV-G protein was not seen inside the tubules (arrowheads in Figure 2B). Together, our results indicate that temperature-induced tubules do not contain cargo.

Analysis of the formation of low temperature-induced Golgi tubules

As reported above, 15ºC incubation induced the formation of Golgi-derived long tubules that contain glycosylation enzymes but not matrix or cargo proteins. We next carried out a number of pharmacological treatments in order to define the characteristics of the movement of Golgi proteins at 15ºC (Table I, Figures 3 and 4).

One possibility could be that these low temperature-induced tubules are caused by newly synthesized glycosylation enzymes that leak out the transport block. However, this hypothesis was not supported as the formation of tubules was not inhibited by cycloheximide (data not

shown).

It is well known that the treatment with the drug brefeldin A induces the formation of Golgi tubules and prevents the assembly of COPI coats by inhibition of nucleotide exchange onto ARF (32). These processes result in the rapid redistribution of Golgi enzymes into ER membranes (Figure 3C). Addition of brefeldin A simultaneously or after inducing the low temperature did not prevent the formation of the tubules containing Golgi enzymes. In fact, Golgi-derived tubules were longer and more abundant after the addition of the drug (Figure 3D). However, the characteristic ER-staining pattern for Golgi enzymes caused by BFA treatment in cells cultured at 37ºC was not observed at 15ºC even after long times of incubation (2 hours, data not shown). Thus, the blockade of the membrane traffic at the ERGIC induced by low temperature inhibited the brefeldin A-induced Golgi redistribution into the ER.

Aluminium fluoride activates trimeric G-proteins and enhances the association of COPI coats to Golgi membranes (33). The stabilization of the coat induces vesicle accumulation and transport inhibition. When cells cultured at 37ºC were treated with aluminium fluoride, the Golgi complex was virtually unaltered (Figure 3E). When the cells were cultured at 15ºC, and subsequently treated with this compound, tubules also remained unaltered (Figure 3F, inset). The percentage of cells showing tubular formations (82%) and their appareance were similar to cells cultured at 15ºC without the drug (Table I). Conversely, when aluminium fluoride was added before or simultaneously in cells cultured at 15ºC, the formation of tubules was strongly reduced (Figure 3F). Moreover, not only a lower percentage the cells with tubules was detected (27%), but the number of tubules, their length and thickness were also reduced (Table I). Therefore, aluminium fluoride treatment inhibits the formation of Golgi tubules induced by low temperature but it cannot reverse this process.

We next examined the requirement of energy. Energy can be depleted by addition of

sodium azide and deoxyglucose (34). In our system, energy depletion had similar effects to those of aluminium fluoride, albeit weaker (Figures 3G and 3H).

Finally, we also investigated the involvement of cytoskeleton in the low temperature-induced Golgi tubulation process (Figure 4). Nocodazole inhibits polymerisation of tubulin monomers, which results in disruption of microtubules. The nocodazole treatment of HeLa cells at 37ºC resulted in the expected Golgi fragmentation (35; Figure 4A). When cells were cultured at 15ºC, nocodazole produced some Golgi fragmentation but not the formation of tubules (Figure 4B, Table I). The disruption of actin filaments by latrunculin B treatment also inhibited the low temperature-induced Golgi tubulation and Golgi complex compactness (Figure 4C and 4D and Table I; 36,37). Together, these results support that Golgi tubules depend on both microtubular and actin cytoskeletons.

In summary, the formation of Golgi tubules is not originated by de novo synthesis of glycosylation enzymes; it depends on energy and intact cytoskeleton and is sensitive to aluminium fluoride but not to brefeldin A or cycloheximide.

Ultrastructure of the low-temperature induced Golgi tubules

The ultrastructure of the Golgi complex of cells cultured at 15ºC was examined by transmission electron microscopy. The Golgi complex morphology of HeLa cells has been extensively studied and its ultrastructure is not significantly different from that of other cultured cells (38). A typical Golgi stack consisted of 4-7 flattened cisternae, with an average of 4.3 (Table II). However, this number is inferred from 2D images and may be an understimate (see discussion section). In contrast, the Golgi complex of HeLa cells cultured at 15ºC showed significant differences (Figures 5 and 6). Most of the Golgi stacks were much longer (Figures 5E, 6C and 7D). The average length of the cisterna was double that in control cells (Table II). In addition, most stacks

were curved. The average number of cisternae per stack in these cells (5.2) was significantly higher (t-test, p=0.003). Circular Golgi stack were often seen in these cells (Figures 5B and 5E). The diameter and number of cisternae per stack of these round Golgi stacks was similar to characteristic flat stack of cells cultured at 37ºC (Table II). Often, long curved and round types of stack were seen in the same Golgi ribbon (Figure 5E). The Golgi stacks of HeLa cells cultured at 15ºC were surrounded by abundant tubulo-vesicular elements. Tubules (30-60 nm thick) were often seen in these cells (Figures 5C-E). We also observed tubules directly connected with cisternae (Figure 5C). The tubules may occasionally appear connected each other forming large structures of huge complexity adjacent to the stack (Figure 5E).

We studied the Golgi distribution of glycosyltransferases at 15ºC by quantitative immunoelectron microscopy. We chose GalTr since ManII and GalNAcTr antibodies gave a very weak signal in HeLa cells and therefore they were not suitable for quantitative ultrastructural analysis. The distribution of GalTr in HeLa cells has been extensively studied (39,40). Accordingly, we also found that GalTr was restricted to trans cisternae (Figure 5A, Table III). However, the distribution of GalTr was significantly modified in cells cultured at 15ºC (Figures 5B-E). In most of the cells examined, GalTr appeared evenly distributed across the Golgi stack (Figures 5B and 5C, Table III). The changes in the distribution of GalTr when temperature was lowered were not observed for more stable components of the Golgi complex such as matrix proteins (Figure 6, Table III).

GalTr immunolabelling was not restricted to cisterna in control cells but a significant percentage (23%) of this Golgi-resident enzyme was visualized in tubulo-vesicular elements adjacent to the Golgi stack (Table III, see also reference 40). It has been suggested that these membranes represent the TGN but GalTr does not colocalize with TGN46 (40). Low temperature increased three-fold the percentage of labelling outside of the cisterna (Table III). Many of these

elements were tubular and appeared connected to the stack (Figures 5C and 5E). They most likely corresponded to the tubular extensions observed at light microscopy. Immunolabelled tubules at the cell periphery were also observed (Figure 5D). These tubules were very similar to trans Golgi network membranes (TGN) but they were devoid of TGN46 (data not shown).

Membrane dissociation of COPI coat complexes at 15ºC

COPI multiprotein coat complexes has been involved in the formation of Golgi tubules (see discussion). Therefore, we next examined whether low temperature culture conditions perturb their membrane dynamics. In control cells, β-COP component of the COPI coat complexes was localized by immunofluorescence to the perinuclear Golgi area and in punctate structures distributed throughout the cytoplasm (Figure 7A). In contrast, at 15ºC they detached from Golgi membranes and were redistributed in the cytoplasm (Figure 7B). This result was confirmed by cryoimmunoelectronmicroscopy (Figure 7C and 7D). Quantitative analysis showed that the percentage of membrane-associated labelling decreased from 66% to 29% when temperature was shifted from 37ºC to 15ºC. This redistribution started after 5 min at 15ºC and increased thereafter. Thus, the percentage of cells showing cytoplasmic labelling after 5 min, 15 min, 30 min, 1 h and 3 h was 21, 59, 77, 87 and 96%, respectively. However, perinuclear Golgi-like labelling did not completely disappear until 3 h of treatment (Figure 7B). Together, these data strongly suggest a direct relationship between COPI dissociation from membranes and tubular formation.

DISCUSSION

In the present study, we report that the blockade of protein transport when cells are incubated at 15ºC induces the formation of Golgi-derived tubules. These tubules contain Golgi-resident glycosylation enzymes but not Golgi matrix proteins. They also lack anterograde (VSV-G) and

retrograde (Shiga toxin) cargo. Tubules are a common feature of the secretory pathway (41,42), which have been observed either in ERGIC/cis Golgi network and TGN. Furthermore, tubular connections between the stacks which constitutes the Golgi ribbon are often described. Tubular connections between the ER and ERGIC and between cisternae of the same stack although rare have also been described in some cell types (43). BFA-induced tubules rise from Golgi and fuse with ER membranes and are microtubule- and energy-dependent (32). Low temperature (15ºC)-induced tubules are dependent on energy and microtubule but, unlike BFA, on microfilaments as well. The latter have been implicated in retrograde (Golgi-to-ER) but not anterograde (ER-to-Golgi) protein transport (36). Low temperature prevents the fusion of Golgi into ER but not the formation of tubules that remain formed after two hours in the presence of BFA. Therefore, the formation of BFA-induced tubules and their subsequent fusion with ER membranes are separate processes. The mechanism of membrane fusion (e.g. SNARE proteins) may be temperature dependent. The best known biochemical change induced by brefeldin A is the release of COPI coats from the Golgi membranes (32). In contrast, aluminium fluoride has the opposite effects: it enhances the association of COPI with membranes (33). It has been suggested that COPI coats prevent tubularization (44). Lowering the temperature affects the mode of the COPI association with Golgi membranes. Thus, we observed that a high percentage of COPI shift to the cytosol at 15ºC. Interestingly, COPI redistribution showed the same kinetics as tubular formation. Thus, both processes begin very soon after temperature lowering and increase thereafter. We postulated that this redistribution frees (uncaps) the rims of the cisternae and it could induces tubulation. Tubules, however, were not observed in all cell types (the present study; 25). The redistribution of COPI may be cell type-dependent which could explain why not all clonal cell lines form tubules when cultured at 15ºC. The role of COPI coat complex in retrograde transport is well established but its role in anterograde transpport is controversial (4,5,45). In addition, it has been

shown that maturation of ERGIC elements required the exchange of anterograde cargo-depleted of COPI coats (46). If COPI mediates ERGIC-to-Golgi transport, its dissociation from these membranes could explain the block at the ER/Golgi interface. However, this blockade could be indirect. Thus, a block in the retrograde pathway may block the anterograde route because the molecular machinery necessary is not recycled.

Our finding that low temperature increases the length of stacks of HeLa cells is the opposite of that reported in hepatoma cells (25). Our electron microscopy study strongly suggests that temperature induces the fusion of different stacks of the Golgi ribbon. Tubules have been implicated in lateral mixing of organelles (homotypic fusion) whereas heterotypic fusion between organelles could require coat complexes (32). Our results suggest that low temperature increases the formation of Golgi-derived tubules. Some of these tubules might connect different stacks to form larger Golgi complexes. Other tubules, however, may not contact with other membranes so that they extent further to the cell periphery. On the other hand, the number of cisternae per stack also increases at 15ºC. It is difficult to count cisternae from 2D images (38). Cis- and trans-most cisternae are quite fenestrated and cannot be unambiguously differentiated from adjacent tubulovesicular membranes. Thus, our data may not necessarily indicate a change in the number of cisternae but a modification in their structure. After temperature lowering cis/trans cisternae may show fewer fenestrations so that they can then be identified as a characteristic stacked Golgi cisterna.

Low temperature also changed the shape of the Golgi stack. The stacks of cells cultured at 37ºC are typically flatten or slightly curved. However, the stack of cells cultured at 15ºC are very curved and often completely circular. These changes in morphology cannot be explained by the simple alteration of the microtubule cytoskeleton caused by low temperature. Treatment of cells with the microtubule-disrupting agent nocodazole had the opposite effect, i.e. Golgi

fragmentation and its subsequent reformation as a ministacks (35). The only similarity we found is the appearance of onion-like Golgi structures. However, GalTr remained polarized on nocodazole-induced round Golgis but not in those induced at 15º, where this enzyme was evenly distributed across the stack. The morphology of the stacks at 15ºC is also different from cells cultured at 20ºC. This temperature condition blocks the secretory pathway at the TGN. The most significant characteristic of the stacks at 20ºC is the presence of large bulging domains on the trans cisternae (47).

One of the most intriguing characteristics of the Golgi complex is its morphological and functional polarization. This is true for many components including resident enzymes and matrix proteins. In fact, it was the main observation that led to the stationary cisterna (vesicular) model for intraGolgi transport (1). However, this observation can also be explained by the cisternal maturation model, according to which Golgi components are kept in place by the selective recruitment of COPI vesicles (48). Golgi proteins with high and low affinity for COPI will be preferentially located on the cis and trans side, respectively. This model explains why polarization is not absolute and Golgi proteins showed a gradient-like rather than a sharp distribution (13,49). We found that enzymes but not matrix proteins lose their polarized distribution at 15ºC. The loss of the Golgi polarity within the stack at low temperature could be explained by heterotypic fusion mediated by tubules between cisternae of different stacks of the Golgi ribbon. If this fusion occurs randomly it will induce a mixture of Golgi components. Given that Golgi tubules only contain glycosylation enzymes, the loss of polarity would affect only these molecules and not matrix protein, which are prevented from entering the tubules.

What could be the functional role of the Golgi-derived tubules? It has been postulated that Brefeldin A-induced tubules could be involved in Golgi-to-ER transport. Thus, the use of this drug revealed a physiological process. It may be the case when secretory transport is blocked at

15ºC. The fact that the low temperature-induced tubules only contain Golgi-resident glycosylation enzymes suggests a role for Golgi-derived tubules in their recycling at the ER/Golgi interface. The cisternal maturation model for intraGolgi transport postulates that Golgi enzymes move backwards within vesicles to avoid their lost and to keep the polarity of the stack (13). However, it cannot be excluded that the recycling of Golgi enzymes could be mediated by tubules. In fact, vesicles cannot be unambiguously distinguished from tubules on EM cryosections (50). Conversely, it is clear from our results that Golgi matrix proteins demonstrated here with GM130, golgin-84 and giantin, are excluded from these tubules, which indicates that the recycling of these proteins is mediated by other mechanisms (vesicles or cytoplasmic diffusion).

In conclusion, we postulate that low temperature has primary effect over coat complex COPI. It dissociates from endomembranes inducing the blockade at ERGIC and the formation of Golgi emerging tubules.

MATERIALS AND METHODS

Antibodies and reagents

Monoclonal antibody GTL2 against galactosyltransferase (GalTr) was provided by Dr T. Suganuma (Miyazaki Medical College, Miyazaki, Japan). The two polyclonal antibodies against mannosidase II (Man II) were obtained from Dr. K. Moremen (University of Georgia, Athens, GA, USA) and Chemicon International Inc (Temecola, CA, USA). Monoclonal antibody against N-acetyl-galactosaminyltransferase (GalNAcTr) T2 was obtained from Dr H. Clausen (University of Copenhagen, Copenhagen, Denmark). Monoclonal antibody against giantin was provided by Dr. H.-P Hauri (University of Basel, Basel, Switzerland). Polyclonal antibody against Golgi-84 was from Dr. G. Warren (Yale University, New Haven, CT, USA). Monoclonal

P5D4 anti-VSV-G protein and M3A5 anti-β-COP antibodies were purchased from Sigma Chemicals Co (San Louis, MO, USA). Sheep anti-human antibody TGN46 was from Serotec (Oxford, U.K.) and monoclonal antibody against GM130 from BD Transduccion Laboratories (Erembodegem, Belgium). FITC/TRITC-conjugated secondary antibodies and the rabbit anti-mouse antibody were from Dako A/S (Glostrup, Denmark). Rabbit anti-sheep antibodies were from Molecular Probes (Eugene, OR, USA). Protein A-gold was obtained from the Department of Cell Biology at Utrecht University (Utrecht, The Netherlands). Cell culture media were obtained from Gibco BRL Life Technologies (Paisley, Scotland, UK). Cycloheximide was from ICN (VB Amsterdam, The Netherlands). Latrunculin B was obtained from Calbiochem (Damrmstadt, Germany). Brefeldin A, TRITC-phallodin, nocodazole, 2-deoxy-D-glucose, sodium azide and unspecified chemical reagents were purchased from Sigma.

Cell culture and temperature lowering

Cell lines were cultured in D-MEM supplemented with 10% FBS, 100 i.u./ml penicillin/streptomycin and 100 μg/mL glutamine under standard tissue culture conditions (37ºC, 5% CO_2). For the temperature experiments, cells were cultured in a temperature controlled incubator at 15ºC for 3 h, unless specified. Where indicated, cells were treated with aluminium fluoride (50 μM $AlCl_3$ and 30mM NaF), brefeldin A (1 μg/ml), nocodazole (25 μM), latrunculin B (400 nM), 2-deoxy-D-glucose (50 mM) and sodium azide (0.05%) (energy depletion) or cycloheximide (20 μgr/ml). The experimental conditions for each reported experiment are indicated in Table I.

Immunofluorescence microscopy

Cells grown on coverslips were quickly fixed with 4% paraformaldehyde in PBS or cold (-20ºC)

methanol, permeabilized with 0.1% saponine and processed for indirect immunofluorescence. Polyclonal and monoclonal antibodies were visualized with TRITC or FITC-conjugated anti-rabbit, anti-mouse or anti-sheep secondary antibodies. Samples were examined with a Zeiss Axiophot fluorescent microscope or under a Leica TCS SP2 confocal microscope. Images were assembled using Adobe Photoshop version 6.0.

Quantitation of the percentage of cells immunolabelled for GalNAcTr showing tubules was performed by analysing 100-200 cells per treatment (Table I).

VSV-G and Shiga toxin B transport assays

Shiga toxin was used as a physiological marker of the retrograde pathway since is transported to the ER via early/recycling endosomes and the Golgi complex (51). The transport of the toxin was monitored by immunofluorescence as described previously (36). The cells were incubated with Cy3-labelled fragment B of the Shiga toxin at 4ºC. Cells were maintained at 37ºC for 2 h. At this time period, Shiga toxin accumulates at the Golgi complex. Finally, cells were cooled to 15ºC for different times in order to induce the formation of tubules (see results).

Virus infection with the temperature-sensitive mutant ts045 and indirect immunofluorescence assay of the anterograde transport of VSV-G were performed as described previously (36). Briefly, cells monolayers were infected with the mutant virus in D-MEM without serum at 32ºC and then incubated for 2h of at the non-permissive temperature (40ºC) in the same culture medium plus FCS. The cells were maintained another 30 min at this temperature in the presence of cycloheximide. Then, the temperature was raised to 32ºC for 10 min. Finally, the temperature was shift to 15ºC to monitor tubular formation.

Quantitative immunoelectron microscopy

HeLa cells cultured at 37ºC or 15ºC were fixed with 2% paraformaldehyde and 0.2% glutaraldehyde in 0.1 M sodium phosphate buffer, pH 7.4. After washing in buffer, the cells were pelleted by centrifugation, embedded in 10% gelatin, cooled on ice and cut into 1 mm^3 blocks. The blocks were infused with 2.3 M sucrose at 4^{o}C overnight, frozen in liquid nitrogen and stored until cryoultramicrotomy. Sections (~50 nm-thick) were cut at -120^{o}C with a diamond knife in a Leica Ultracut T/FCS. Ultrathin sections were picked up in a mix of 1.8% methylcellulose and 2.3 M sucrose (1:1) according to Liou et al. (52). Cryosections were collected on carbon and formvar-coated copper grids and incubated with rabbit polyclonal antibodies followed by protein A-gold (53). Rabbit anti-mouse immunoglobulins antibodies were used as bridging antibodies when monoclonal antibodies were used. After labelling, the sections were treated with 1% glutaraldehyde, counterstained with uranyl acetate pH 7 and embedded in methyl cellulose-uranyl acetate pH 4 (9:1) (54,55). Grids were examined with a Philips Tecnai 12 electron microscope.

To study the length and number of cisternae per Golgi stack in cells cultured at 37ºC and 15ºC the highest quality cryosections were selected and photographed at 18,000-26,000x (Table II).

The cis-trans Golgi distribution of GalTr and GM130 was calculated over 25 cross-sectioned Golgi stacks of cells cultured at 37ºC or 15ºC showing an unambiguous cis-trans polarity using the criteria previously described (11). Cisternae were numbered from cis (G1) to trans (G5) as described (13). The number of gold particles found in each cisterna were counted and expressed as percentage of the total (Table III).

ACKNOWLEDGMENTS

We are grateful to Drs Suganuma, Hauri, Warren, Moremen, and Clausen for providing antibodies against GalTr, giantin, golgin 84, mannosidase II and GalNAcTr, respectively. We thank M.C. González-Ulloa for excellent photographic assistance. E.M.A was supported by predoctoral fellowships from Ministerio de Educación, Cultura y Deporte. This work has been supported by grants from Ministerio de Ciencia y Tecnología to J.B (BMC2003-03738), G.E. (BMC2003-01064) and J.A.M-M. (BFU2004-05568/BFI) and Fundación Séneca to J.A.M-M. (PB/49/FS/02)

REFERENCES

1. Farquhar MG, Palade, GE. The Golgi Apparatus (complex)- from artefact to center stage. J Cell Biol 1981;91, 77s-103s.

2. Farquhar MG, Hauri HP. Protein sorting and vesicular traffic in the Golgi apparatus. In: The Golgi apparatus, Berger E, Roth J, editors. Basel, Switzerland: Birkhäuser Verlag; 1997. p 63-128.

3. Bannykh SI, Balch WE. Membrane dynamics at the endoplasmic reticulum-Golgi interface. J Cell Biol 1997;138,1-4.

4. Glick BS. Organization of the Golgi apparatus. Curr Opin Cell Biol 2000;12, 450-456.

5. Klumperman J. Transport between ER and Golgi. Curr Opin Cell Biol 2000;12, 445-449.

6. Lippincott-Schwartz J, Roberts TH, Hirschberg K. Secretory protein trafficking and organelle dynamics in living cells. Annu Rev Cell Dev Biol 2000;16, 557-589.

7. Bannykh SI, Rowe T, Balch WE. The organization of endoplasmic reticulum export complexes. J Cell Biol 1996;135, 19-35.

8. Hauri H.-P, Schweizer A. The endoplasmic reticulum-Golgi intermediate compartment. Curr Opin Cell Biol 1992;4, 600-608.

9. Hauri H.-P, Kappeler F, Andersson H, Appenzeller C. ERGIC-53 and traffic in the secretory pathway. J Cell Sci 2000;113, 587-596.

10. Allan BB, Balch WE. Protein sorting by direct maturation of Golgi compartments. Science 1999;285, 63-66.

11. Bonfanti L, Mironov Jr AA , Martínez-Menárguez JA, Martella O, Fusella A, Baldassare M, Buccione R, Geuze HJ, Mironov AA, Luini. A. Transport of procollagen across the Golgi stack is progressive maturation of Golgi cisternae. Cell 1998;95, 993-1003.

12. Volchuk A, Amherdt M, Ravazzola M, Brugger B, Rivera VM, Clackson T, Perrelet A, Sollner TH, Rothman JE, Orci L. Megavesicles implicated in the rapid transport of intracisternal aggregates across the Golgi stack. Cell 2000;102, 335-48.

13. Martinez-Menarguez JA, Prekeris R, Oorschot VM, Scheller R, Slot JW, Geuze HJ, and Klumperman J. Peri-Golgi vesicles contain retrograde but not anterograde proteins consistent with the cisternal progression model of intra-Golgi transport. J Cell Biol 2001;155, 1213-1224.

14. Cosson P, Amherdt M, Rothman JE, Orci L. A resident Golgi protein is excluded from peri-Golgi vesicles in NRK cells. Proc Natl Acad Sci USA 2002;99, 12831-12834.

15. Zaal KJM, Smith CL, Polishchuk RS, Altan N, Cole NB, Ellenberg J, Hirschberg K, Presley JF, Roberts TH, Siggia E, Phair RD, Lippincott-Schwartz. J. Golgi membranes are absorbed into and reemerge from the ER during mitosis. Cell 1999;99, 589-601.

16. Shorter J, Warren G. Golgi architecture and inheritance. Annu Rev Cell Dev Biol. 2002;18:379-420.

17. Pecot MY, Malhotra V. Golgi membranes remain segregated from the endoplasmic reticulum during mitosis in mammalian cells. Cell 2004;116, 99-107.

18. Rothman JE, Wieland FT. Protein sorting by transport vesicles. Science 1996;272, 227-234.

19. Lippincott-Schwartz J, Donaldson JG, Schweizer A, Berger EG, Hauri H-P, Yuan LC, Klausner RD. Microtubule-dependent retrograde transport of proteins into the ER in the presence of brefeldin A suggest an ER recycling pathway. Cell 1990;60, 821-836.

20. Horstmann H, Ng CP, Tang BL, Hong W. Ultrastructural characterization of endoplasmic reticulum-Golgi transport containers (EGTC). J Cell Sci 2002;115, 4263-4273.

21. Mironov et al.. (13 authors). ER-to-Golgi carriers arise through direct en bloc protrusion and

multistage maturation of specialized ER exit domains. Dev Cell 2003;5, 583-594.

22. Polishchuk RS, Polishchuk EV, Marra P, Alberti S, Buccione R, Luini A, Mironov AA. Correlative light-electron microscopy reveals the tubular-saccular ultrastructure of carriers operating between Golgi apparatus and plasma membrane. J Cell Biol 2000;148, 45-58.

23. Saraste J, Kuismanen E. Pre- and post-Golgi vacuoles operate in the transport of Semliki forest virus membrane glycoproteins to the cell surface. Cell 1984;38, 535-549.

24. Lotti LV, Torrisi MR, Pascale MC, Bonatti S. Immunocytochemical analysis of the transfer of vesicular stomatitis virus G glycoprotein from the intermediate compartment to the Golgi complex. J Cell Biol 1992;118, 43-50.

25. Klumperman J, Schweizer A, Clausen H, Tang BL, Hong W, Oorschot V, Hauri H.-P. The recycling pathway of protein ERGIC-53 and dynamics of the ER-Golgi intermediate compartment. J Cell Sci 1998;111, 3411-3425.

26. Velasco A, Hendricks L, Moremen KW, Tulsiani DRP, Touster O, Farquhar MG. Cell type-dependent variations in the subcellular distribution of a-mannosidase I and II. J Cell Biol 1993;122, 39-51.

27. Kawano J, Ide S, Oinuma T, Suganuma T. A protein-specific monoclonal antibody to rat liver beta 1→4 galactosyltransferase and its application to immunohistochemistry. J Histochem Cytochem 1994;42, 363-369.

28. Rottger S, White J, Wandall HH, Olivo JC, Stark A, Bennett EP, Whitehouse C, Berger EG, Clausen H, Nilsson T. Localization of three human polypeptide GalNAc-transferases in HeLa cells suggests initiation of O-linked glycosylation throughout the Golgi apparatus. J Cell Sci 1998;111, 45-60.

29. Seemann J, Jokitalo EJ, Warren G. The role of the tethering proteins p115 and GM130 in transport through the Golgi apparatus in vivo. Mol Biol Cell 2000;11, 635-645.

30. Diao A, Rahman D, Pappin DJC, Lucocq J, Lowe M. The coiled-coil membrane protein golgi-84 is a novel rab effector required for Golgi ribbon formation. J Cell Biol 2003;160, 201-212.

31. Satoh A, Wang Y, Malsam J, Beard MB, Warren G. Golgin-84 is a rab1 binding partner involved in Golgi structure. Traffic 2003;4:153-161.

32. Klausner RD, Donaldson JG, Lippincott-Schwartz J. Brefeldin A: insights into the control of membrane traffic and organelle structure. J Cell Biol 1992;116, 1071-1080.

33. Donaldson JG, Kahn RA, Lippincott-Schwartz J, Klausner RD. Binding of ARF and beta-COP to Golgi membranes: possible regulation by a trimeric G protein. Science 1991;254, 1197-1199.

34. Oprins A, Duden R, Kreis TE, Geuze HJ, Slot JW. Beta-COP localizes mainly to the cis-Golgi side in exocrine pancreas. J Cell Biol 1993;121, 49-59.

35. Storrie B, White J, Röttger S, Stelzer EHK, Suganuma T, Nilsson T. Recycling of Golgi-resident glycosyltransferase through the ER reveals a novel pathway and provides an explanation for nocodazole-induced Golgi scattering. J Cell Biol 1998;143, 1505-1521.

36. Valderrama F, Duran JM, Babia T, Barth H, Renau-Piqueras J, Egea G. Actin microfilaments facilitate the retrograde transport from the Golgi complex to the endoplasmic reticulum in mammalian cells. Traffic 2001;2: 717-726

37. Valderrama F, Babia T, Ayala I, Kok JW, Renau-Piqueras J, Egea G. Actin microfilaments are essential for the cytological positioning and morphology of the Golgi complex. Eur J Cell Biol 1998;76, 9-17.

38. Ladinsky MS, Mastronarde DN, McIntosh JR, Howell KE, Staehelin LA. Golgi structure in three dimensions: functional insights from the normal rat kidney cell. J Cell Biol 1999;144, 1135-1149.

39. Roth J, Berger EG. Immunocytochemical localization of galactosyltransferase in HeLa cells: codistribution with thiamine pyrophosphatase in trans-Golgi cisternae. J Cell Biol 1982; 93, 223-229.

40. Prescott AR, Lucocq JM, James J, Lister JM, Ponnambalam S. Distinct compartmentalization of TGN46 and beta 1,4-galactosyltransferase in HeLa cells. Eur J Cell Biol 1997;72, 238-246.

41. Mironov AA, Weidman P, Luini A. Variations on the intracellular transport theme:maturing cisternae and trafficking tubules. J Cell Biol 1997;138, 481-484.

42. Mollenhauer HH, Morré DJ. The tubular network of the Golgi apparatus. Histochem Cell Biol 1998;109, 533-543.

43. Clermont Y, Rambourg A, Hermo L. Connections between the various elements of the cis- and mid-compartments of the Golgi complex of early rat spermatids. Anat Rec 1994;240, 469-480.

44. Kreis TE. Regulation of vesicular and tubular membrane traffic of the Golgi complex by coat proteins. Curr Op Cell Biol 1992;4, 609-615.

45. Orci L, Stamnes M, Ravazzola M, Amherdt M, Perrelet A, Söllner TH, Rothman JE. Bidirectional transport by distinct populations of COPI-coated vesicles. Cell 1997;90, 335-349.

46. Shima DT, Scales SJ, Kreis TE, Pepperkok R. Segregation of COPI-rich and anterograde-cargo-rich domains in endoplasmic-reticulum-to-Golgi transport complexes. Curr Biol 1999;9: 821-824.

47. Ladinsky MS, Wu CC, McIntosh S, McIntosh JR, Howell KE. Structure of the Golgi and distribution of reporter molecules at 20 degrees C reveals the complexity of the exit compartments. Mol Biol Cell 2002;13, 2810-2825.

48. Glick BS, Elston T, Oster G. A cisternal maturation mechanism can explain the asymmetry of the Golgi stack. FEBS Lett 1997;414, 177-181.

49. Rabouille C, Hui N, Hunte F, Kieckbusch R, Berger EG, Warren G, Nilsson T. Mapping the distribution of Golgi enzymes involved in the construction of complex oligosaccharides. J Cell Sci 1995;108, 1617-1627.

50. Kweon H.-S, Beznoussenko GV, Micaroni M, Polishchuk RS, Trucco A, Martella O, Di Giandomenico D, Marra P, Fusella A, Di Pentima A, Berger EG, Geerts WJC, Koster AJ, Burger KNJ, Luini A, Mironov AA. Golgi enzymes are enriched in perforated zones of Golgi cisternae but are depleted in COPI vesicles. Mol. Biol Cell 2004; in Press.

51. Mallard F, Antony C, Tenza D, Salamero J, Goud B, Johannes L. Direct pathway from early/recycling endosomes to the Golgi apparatus revealed through the study of shiga toxin B-fragment transport. J Cell Biol 1998;143, 973-990.

52. Liou W, Geuze HJ, Slot JW. (1996). Improving structural integrity of cryosections for immunogold labelling. Histochem Cell Biol 1996;106, 41-58.

53. Slot JW, Geuze HJ. A new method of preparing gold probes for multiple-labeling

cytochemistry. Eur J Cell Biol 1985;38, 87-93.

54. Slot JW, Geuze HJ, Gigengack S, Lienhard GE, James JE. Immuno-localization of the insulin regulatable glucose transporter in brown adipose tissue of the rat. J Cell Biol 1991;113, 123-135.

55. Martínez-Menárguez JA, Geuze HJ, Slot JW, Klumperman J (1999). Vesicular tubular clusters between the ER and Golgi mediate concentration of soluble secretory protein by exclusion from COPI-coated vesicles. Cell 1999;98, 81-90.

Table I. Effects of different treatments on the number and morphology of GalNAcTr-immunolabelled tubules

TREATMENT	Percentage of cells with tubules	Morphology of the tubules
15ºC (3 h)	89	Long, numerous
15ºC (5 min)	66	Long, numerous
15ºC (15 min)	78	Long, numerous
15ºC (120 min) + 37ºC (5 min)	28	Short, scarce
15ºC (3 h) + CH	73	Long, numerous
15ºC (60 min) + BFA (30 min)	90	Very long, very abundant
15ºC (60 min) + BFA (120 min)	91	Very long, very abundant
[15ºC + BFA] (30 min)	93	Very long, very abundant
15ºC (90 min) + AlF^-_4 (15 min)	82	Long, numerous
[15ºC + AlF^-_4] (20 min)	27	Short, scarce
15ºC (90 min) + energy depletion (15 min)	82	Long, numerous
[15ºC + energy depletion] (20 min)	44	Short, scarce
Nocodazole (30 min) + 15ºC (30 min)	13	Short, scarce
Latrunculin B (15 min) + 15ºC (20 min)	22	Short, scarce

The square brackets indicate that treatment was done simultaneously. The symbol + indicate that treatment was done sequentially. The numbers between parentheses indicate the time of treatment. The numbers in the second column are the percentage of cells showing at least one unambiguously identified tubule. 100-200 cells were counted for each treatment. The third column indicate the appearance of Golgi tubules when present. CH= cycloheximide; BFA= brefeldin A, AlF^-_4= aluminium fluoride.

Table II. Morphological comparison of Golgi stacks of cultured cells at 37ºC and 15ºC

	number of cisternae per stack	length of cisternae (μm)
37ºC	4.3 ± 0.1	0.689 ± 0.077
15ºC	5.2 ± 0.3	1.573 ± 0.168
15ºC (round stacks)	4.0 ± 0.2	0.636 ± 0.032[a]

Numbers represent mean ± SEM (n=25). [a] Diameter of the round Golgi stack instead of the length of their cisternae

Table III. Cis/trans distribution of Golgi proteins

		G1	G2	G3	G4	G5
GalTr	37ºC	3.0 ± 2.2	4.0 ± 1.5	39.7 ± 6.7	46.7 ± 6.6	12.7 ± 6.8
	15ºC	20.0 ± 7.6	14.3 ± 6.6	20.5 ± 7.2	28.3 ± 8.2	27.8 ± 9.3
GM130	37ºC	60.7 ± 6.6	31.2 ± 5.6	7.6 ± 3.8	0.6 ± 0.6	0.0 ± 0.0
	15ºC	60.2 ± 6.4	29.0 ± 6.3	4.3 ± 2.3	6.7 ± 3.0	1.2 ± 1.2

Numbers represent the percentages (mean ± SEM) of the total labelling over the distinct Golgi cisternae. Cisternae were numbered from cis (G1) to trans (G5) direction. 25 Golgis were counted for each antibody and temperature condition.

FIGURE LEGENDS

Figure 1**.** Immunofluorescence analysis of the distribution of Golgi proteins in cells cultured at 37ºC and 15ºC. GalTr (A), GM130 (C) and giantin (E) show a typical perinuclear labelling pattern in control cells.). At 15ºC, cells showed long tubules emerging from the perinuclear area which are immunoreactive for GalTr (B) At 15ºC, the labelling pattern remains perinuclear for GM130 (D) and giantin (F). Bars, 20 μm

Figure 2**.** Analysis of the cargo content of Golgi tubules by double immunofluorescence. Retrograde (A) and anterograde (B) cargo was monitored by immunofluorescence by using Shiga toxin and VSV-G, respectively. In both cases, cargo proteins were allowed to accumulate at the Golgi area as described in material and methods and then the temperature was shifted to 15ºC for 1h. Despite of the intense colocalization of cargo and GalNAcTr at the Golgi area under this condition, Golgi tubules were negative for both types of cargo (arrowheads). Bars, 20 μm

Figure 3**.** Analysis of the formation of Golgi tubules. The labelling pattern for GalNAcTr was studied before and after the addition of brefeldin A (BFA), aluminium fluoride (ALF_4^-) or energy depletion in parallel experiments carried out at 37ºC and 15ºC. GalNAcTr has a perinuclear pattern at 37ºC (A) but shows a high number of tubules at 15ºC (B). BFA induces the redistribution of the Golgi into the ER at 37ºC (C). However, the same treatment performed at 15ºC exaggerates the formation of tubules (D). ALF_4^- (E,F) or energy depletion (G,H) have no major effects on Golgi morphology under control and low temperature. However, aluminium fluoride does not prevent tubular formation when added after the 15ºC treatment (inset). Bars, 20 μm

Figure 4**.** Golgi tubules formation depends on cytoskeleton. The labelling pattern for GalNAcTr was studied after the depolymerisation of microtubular and actin cytoskeleton by nodocodazole (Nz) or latrunculin B (LtB), respectively, in parallel experiments carried out at 37ºC and 15ºC. Control of these experiments are showed in figure 4. Nz induces the fragmentation of the Golgi complex at both control (A) and low temperature (B). No tubules can be seen at both temperature conditions (B). LtB induces the depolymerisation of actin as seen by double labelling with TRICT-phalloidin and the compactation of the Golgi (C). At low temperature, these phenomena are less marked but tubular formation is prevented (D). Bars, 20 μm.

Figure 5. Distribution of GalTr at 37ºC and 15ºC. Ultrathin cryosections were labelled with monoclonal antibodies against the enzyme followed by a rabbit anti-mouse antibody and 10 nm protein A-gold complex. (A) In control HeLa cells, GalTr is restricted to the trans side of the Golgi stack (G). (B) Round Golgi stack showing that the enzyme is present throughout all cisternae. (C) Golgi stack showing a tubule (arrowheads) in connection with the cisternae. (D) Immunoreareactive tubules at the cell periphery. (E) This picture shows a cell with well-developed tubulo-vesicular membranes strongly labelled for GalTr. Asterisk marks a round Golgi stack forming part of the same ribbon. G= Golgi stack. Bars, 250 nm

Figure 6. Localization of GM130 in control and low temperature cultured cells. Ultrathin cryosections were labelled with monoclonal antibodies against GM130 followed by a rabbit anti-mouse antibody and 10 nm protein A-gold complex. (A) Immunolabelling for GM130 is restricted to the cis Golgi side in control cells. (B) The labelling for this matrix protein is restricted to the center of round Golgi. (C) At 15ºC, GM130 remains associated to the first

cisternae and tubulovesicular membranes at the cis Golgi side. Note that there is an increase of the labelling out of the cisternae when compared to control cells. Arrowhead point to cisternae that appears connected each other. G= Golgi stack.Bars, 250 nm

Figure 7. Dissociation of COPI from membranes. Immunofluorescence (A,B) and immunoelectron microscopy (C,D) analysis of the distribution of COPI in cells cultured at 37ºC (A,C) and 15ºC (B,D). (A) COPI give a punctate labelling pattern in control cells with the highest density at the perinuclear region. (B)At 15ºC , COPI shows a cytosolic-like pattern. (C) COPI coat are found at the cis and lateral Golgi sides (D) After temperature lowering COPI is dispersed throughout the cell mostly non-associated to membranes. Note the complex morphology with curved appearance of the stacks (G). Bars, (A,B) 20 μm, (C,D) 250 nm

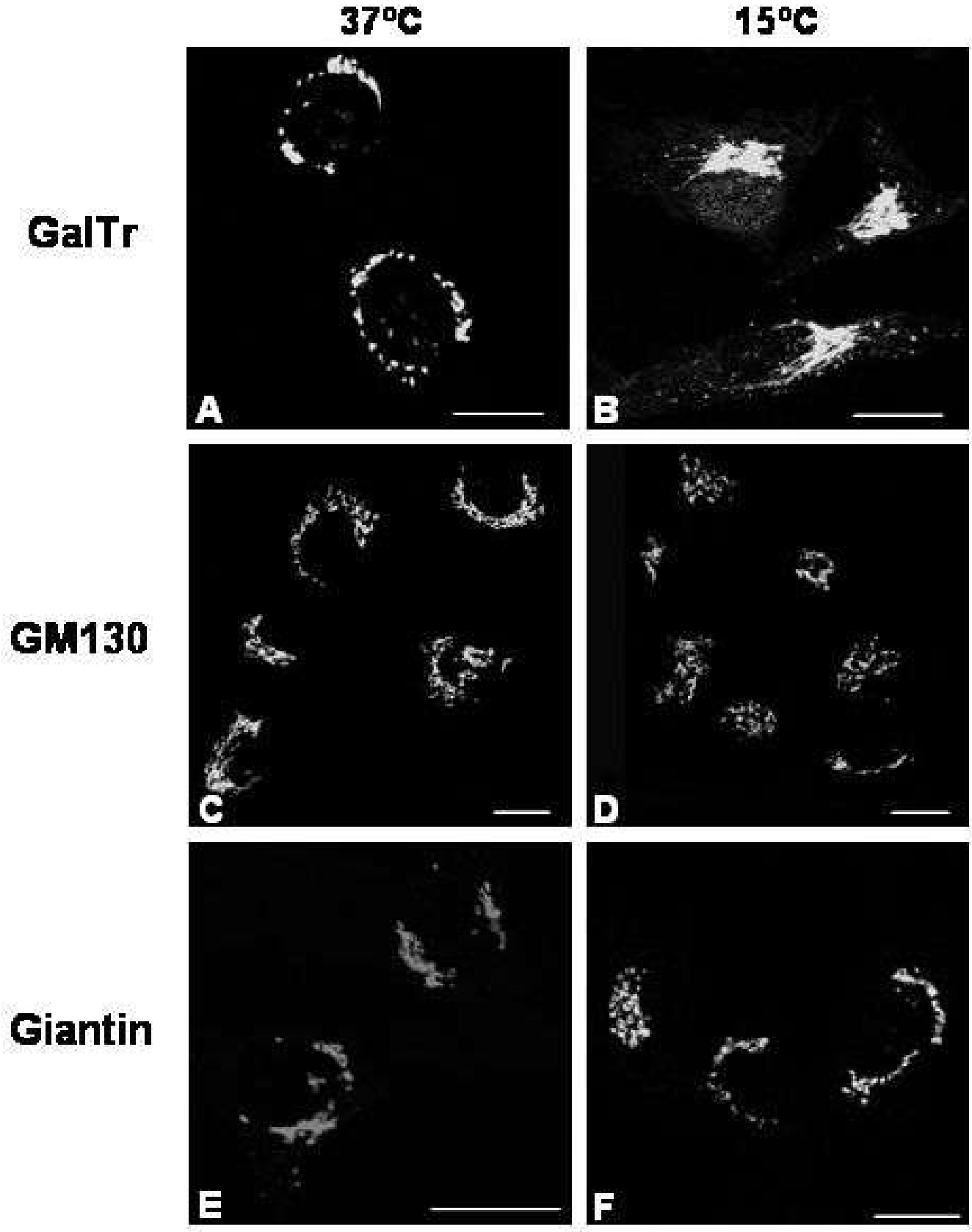
37°C
15°C
GalTr
GM130
Giantin
A
B
C
D
E
F

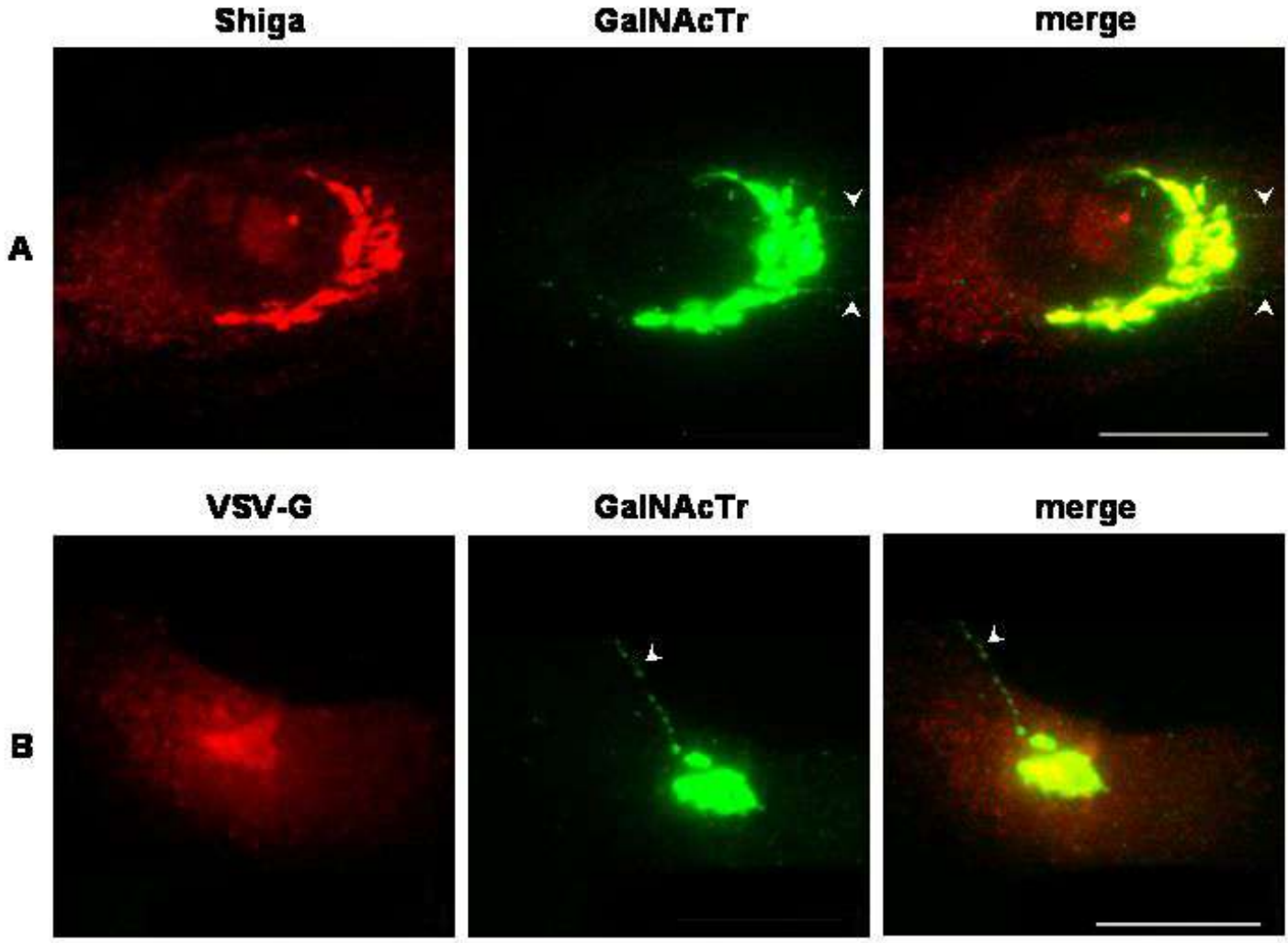
Shiga
GalNAcTr
merge
A
VSV-G
GalNAcTr
merge
B

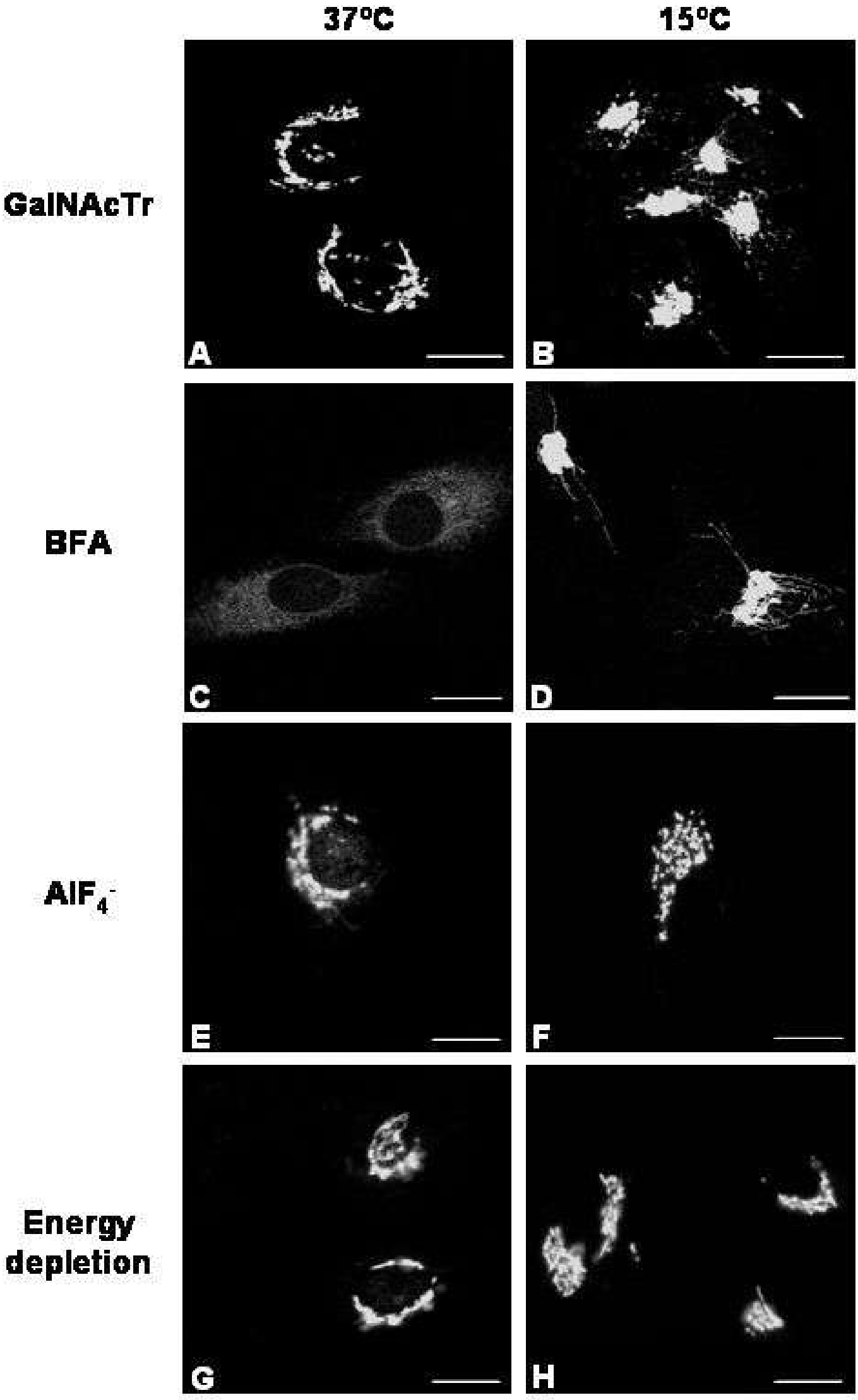
37°C
15°C
GalNAcTr
BFA
AlF_4^-
Energy depletion
A
B
C
D
E
F
G
H

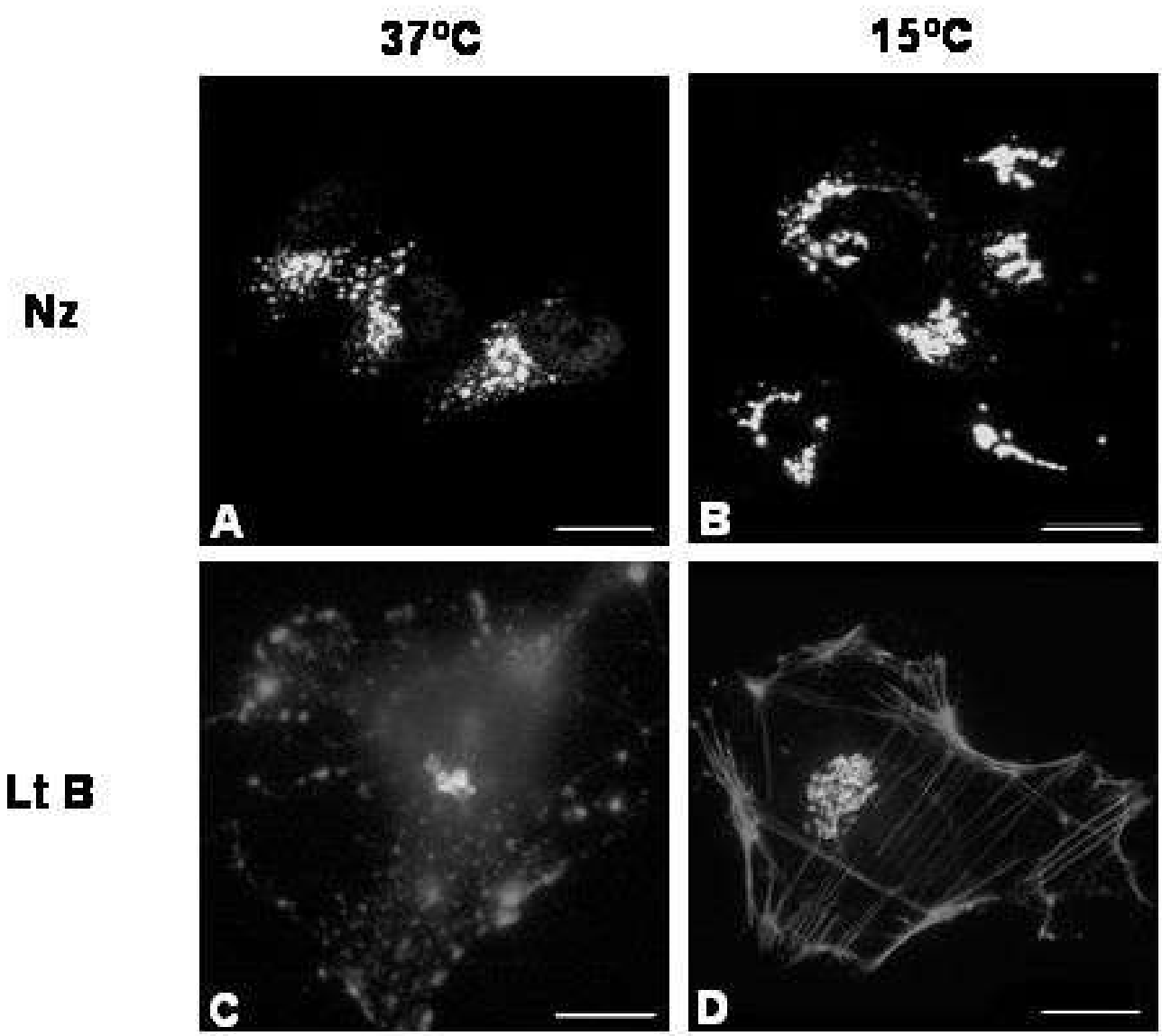
37°C
15°C
Nz
Lt B
A
B
C
D

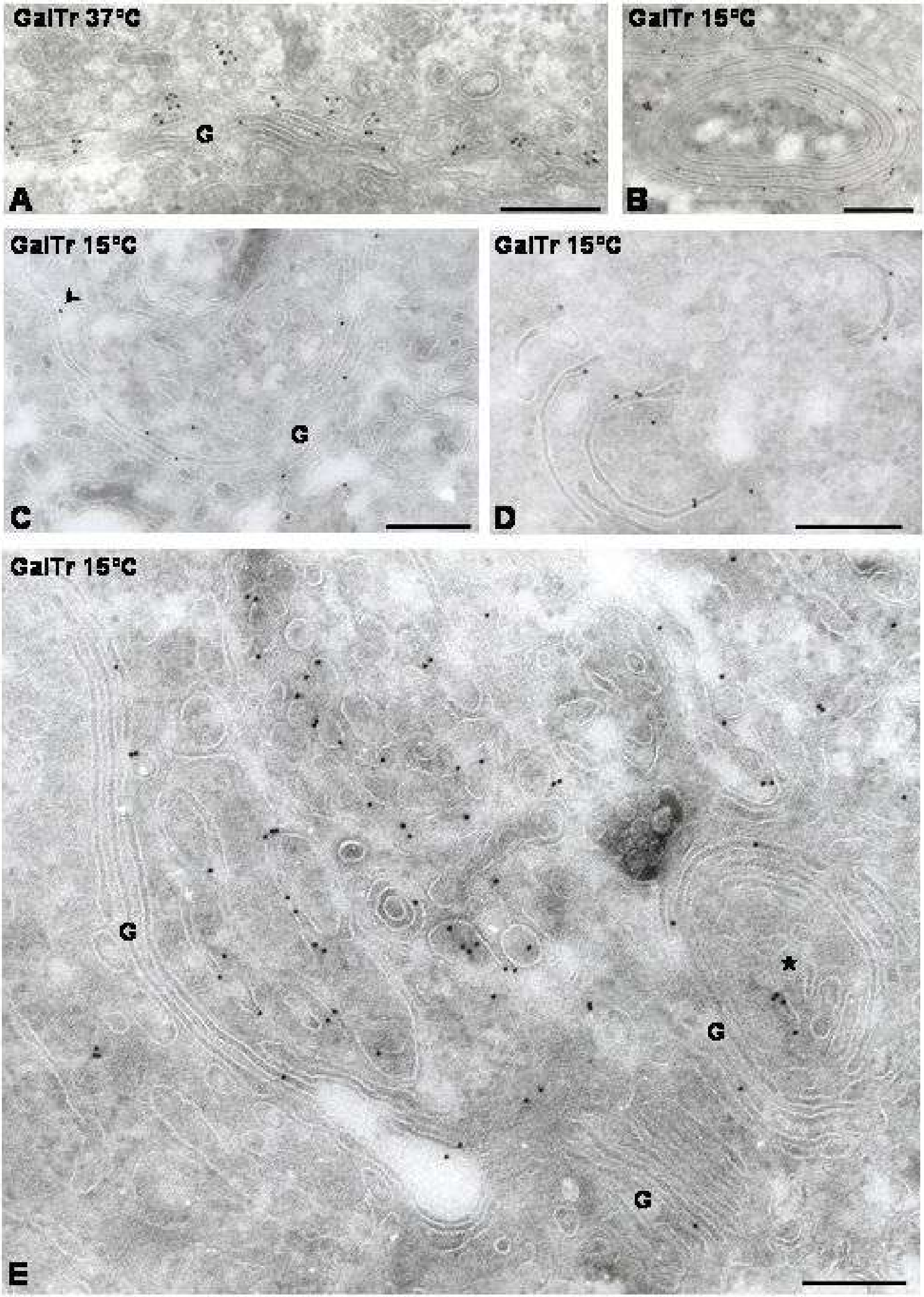
GalTr 37°C
G
A
GalTr 15°C
B
GalTr 15°C
G
C
GalTr 15°C
D
GalTr 15°C
G
G
G
E

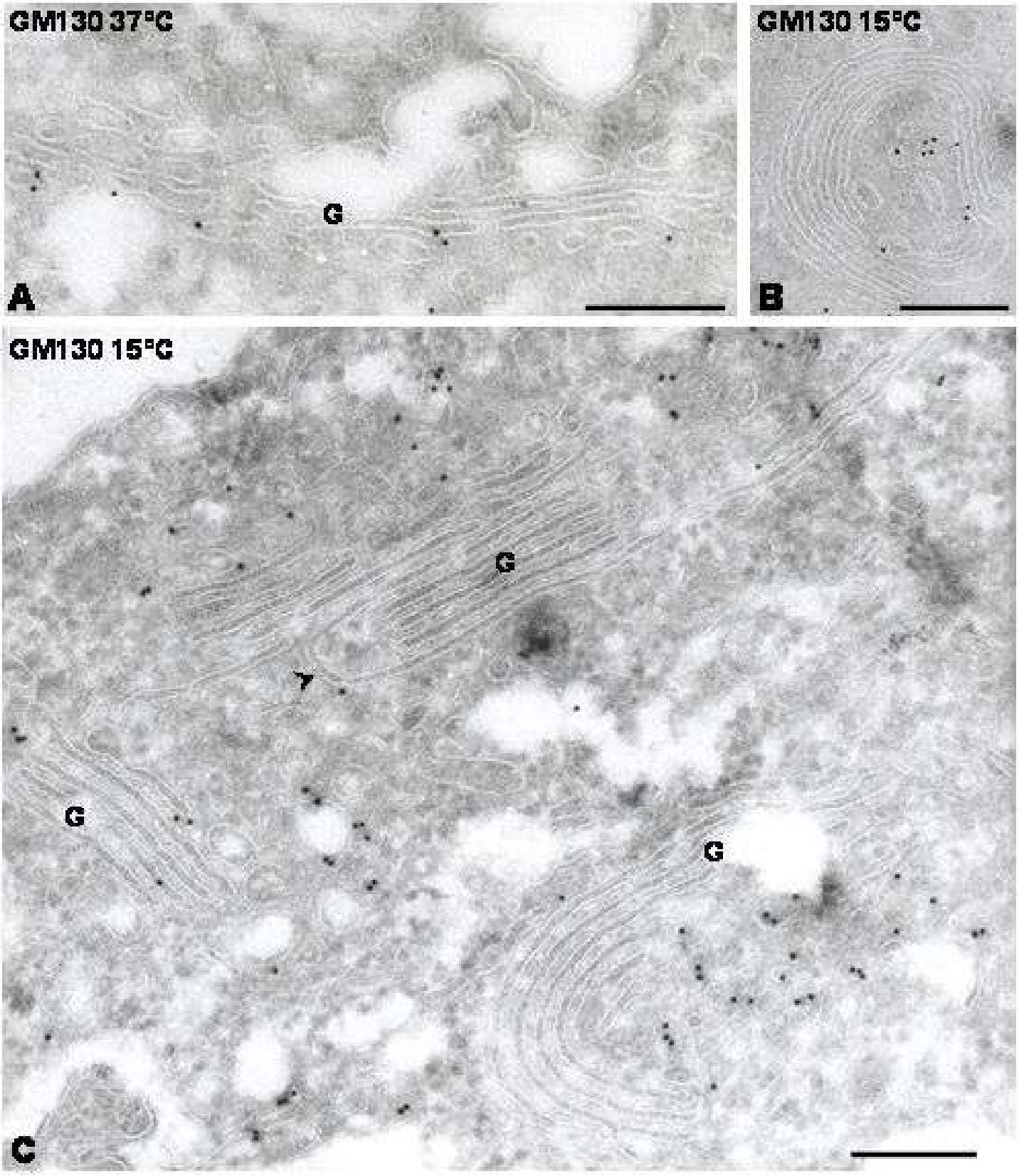
GM130 37°C
G
A
GM130 15°C
B
GM130 15°C
G
G
G
C

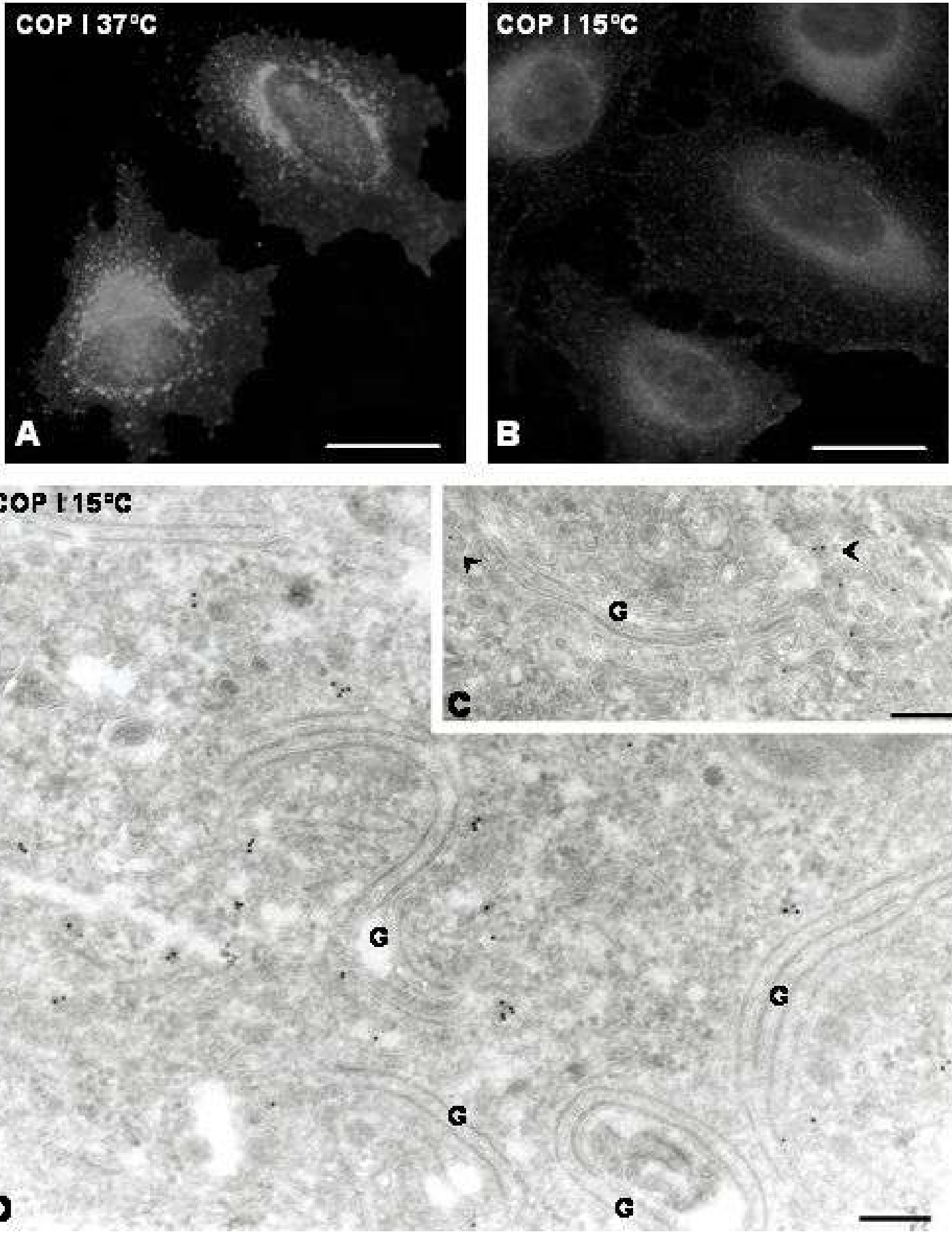
COP I 37°C
A
COP I 15°C
B
COP I 15°C
G
C
G
G
G
G
D